PROCEEDINGS OF SCIENCE

Advancements in Tau Reconstruction and Identification with the CMS experiment

Paola Mastrapasqua[a,*] **on behalf of the CMS Collaboration**

[a] *Centre for Cosmology, Particle Physics and Phenomenology (CP3), UCLouvain, Louvain-la-Neuve, Belgium*

E-mail: paola.mastrapasqua@cern.ch

In recent years, the CMS experiment has achieved significant progress in the reconstruction and identification of hadronically decaying tau leptons, largely driven by advances in machine learning techniques. The current CMS standard employs the Hadron Plus Strips algorithm for hadronic tau reconstruction and the latest DeepTau algorithm, based on Convolutional Neural Networks, for the identification step. This proceeding summarizes these methods and presents a comparison with a novel approach that relies entirely on jet objects. The new method extends existing jet flavor tagging techniques, based on Graph Neural Networks, to also include the identification of hadronically decaying tau leptons. The unified taggers presented here, PNet and UPart, demonstrate several advantages over the traditional approach, while also exhibiting certain limitations. By combining the strengths of old and new algorithms, it is possible to achieve the best identification performance of hadronically decaying tau leptons to date.

The European Physical Society Conference on High Energy Physics (EPS-HEP2025)
7-11 July 2025
Marseille, France

*Speaker

© Copyright owned by the author(s) under the terms of the Creative Commons Attribution-NonCommercial-NoDerivatives 4.0 International License (CC BY-NC-ND 4.0) All rights for text and data mining, AI training, and similar technologies for commercial purposes, are reserved. ISSN 1824-8039 . Published by SISSA Medialab.

https://pos.sissa.it/

PoS(EPS-HEP2025)660

1. The hadrons-plus-strips and DeepTau algorithms

In the standard reconstruction flow used in the CMS experiment at LHC [1], hadronically decaying taus (τ_h) are reconstructed with the hadrons-plus-strips (HPS) algorithm [2, 3]. It is seeded with jets reconstructed by the anti-k_t algorithm [4] with a distance parameter of R=0.4 using particle-flow (PF) candidates [5]. HPS uses the PF candidates near the seeding jet direction of flight to reconstruct the neutral pions that are present in most τ_h decays. The high probability for photons originating from $\pi^0 \to \gamma\gamma$ decays to convert to e^+e^- pairs is accounted for by collecting photons and electrons into clusters ("strips"). The τ_h candidates are then formed by combining the strips with the charged-particles ("prongs") present in the seeding jet and its immediate surroundings. Based on the observed number of strips and charged particles, each τ_h candidate is assigned to different decay modes (DMs). After this reconstruction step, the major challenge is the distinction between genuine τ_h, and quark and gluon jets, which are copiously produced in QCD multijet processes, as well as electrons and muons misidentified as τ_h candidates. For this purpose, the DeepTau identification algorithm [3, 6] has been developed exploiting convolution neural networks to efficiently identify genuine τ_h candidates and reduce the rate of jets, electrons and muons misidentified as τ_h. It exploits a combination of high level input variables and lower-level information from particles around the τ_h flight direction represented in a $\eta \times \phi$ grid format. The network outputs an estimation of the probabilities that a candidate is an electron, a muon, a quark/gluon jet or a genuine τ_h (respectively y_e, y_μ, y_{jet} and y_τ). Finally, these probabilities are used to define the final three discriminators, one for each source of background: $D_\alpha(y) = \frac{y_\tau}{y_\tau + y_\alpha}$ with $\alpha \in \{e, \mu, \text{jet}\}$.

The newest version of the DeepTau algorithm (v2.5) [6] features a refined training workflow which improves classification performance with respect to its predecessor (v2.1) [3], with a reduction of 30–50% in the probability for jets to be misidentified as a τ_h (left panel of Fig. 1). Most interestingly, it includes domain adaptation by backpropagation, a technique that reduces data-to-simulation discrepancies in the region with the highest purity of genuine τ_h candidates. This approach brings the calibration factors used to calibrate the simulation closer to unity, as shown in the right panel of Fig. 1.

2. Unified Jet Taggers: PNet and UPart

In the alternative approach, each jet reconstructed with the anti-k_t algorithm using a distance parameter of $R = 0.4$ is treated as a τ_h candidate, allowing for the recovery of genuine τ_h leptons that are not reconstructed by HPS. The jet candidate can be either a charged-hadron–subtracted (CHS) jet, where pileup is mitigated by removing charged hadrons not originating from the primary vertex [7], or a PUPPI jet, where pileup effects are suppressed using the PileUp Per Particle Identification (PUPPI) algorithm [7–9]. The unified jet taggers provide an inclusive approach to jet flavor and τ_h identification. The latter includes the tasks of τ_h charge and DM assignment. The unified taggers also perform flavor-aware jet energy regression and jet energy resolution estimation. The historically first such tagger is ParticleNet (PNet) [10, 11], a Graph Neural Network architecture that implements the Particle Cloud representation for jets. A more recent algorithm, UParT [12–14], is based on the Particle Transformer architecture. Similarly to PNet, it employs the Particle Cloud

PoS(EPS-HEP2025)660

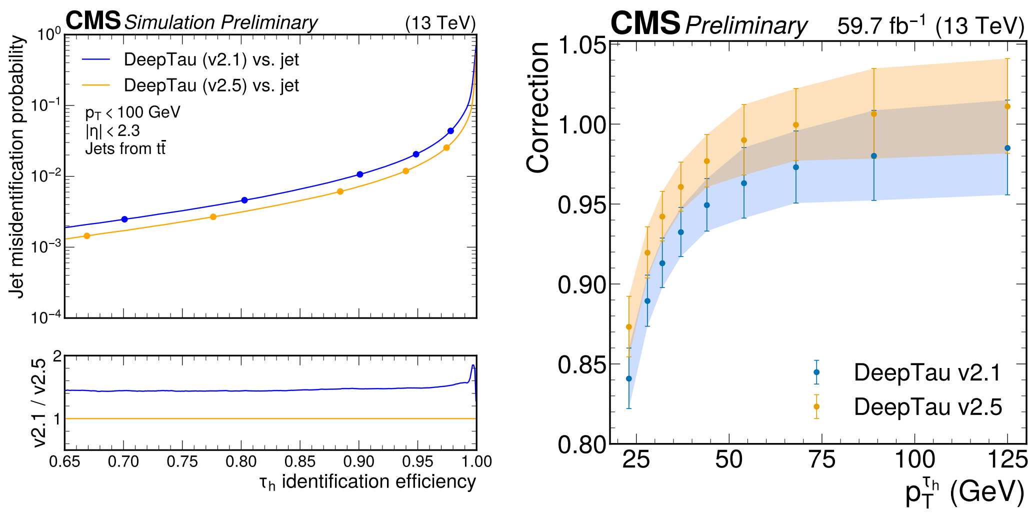

Figure 1: (Left) Jet misidentification probability versus genuine τ_h identification efficiency evaluated on 2018 simulated datasets. The defined working points of the discriminator are indicated as filled circles. (Right) The data-to-simulation calibration factors of the τ_h identification efficiency as functions of p_T in the 2018 data-taking period. The vertical bars correspond to the combined statistical and systematic uncertainties [6].

representation but adds an attention-based mechanism. In addition, UParT incorporates adversarial training to enhance robustness against simulation mismodeling.

3. Comparison of the different approaches

In the following, the performance of the three taggers—DeepTau v2.5, PNet, and UParT—is evaluated and compared in simulation (in Z + jets events), highlighting the complementary strengths of the different approaches [15]. Since the algorithms are originally defined on three distinct reconstructed objects—HPS τ_h candidates, CHS jets, and PUPPI jets—their efficiency and purity are assessed on a unified set of τ_h candidates. This set is defined as the union of all reconstructed objects with $p_T > 20$ GeV, $|\eta| < 2.5$, and $|dz| < 0.2$ cm. The unified collection is constructed by first including HPS τ_h candidates, followed by CHS jets, and then PUPPI jets that do not overlap with previously added candidates. Consequently, by construction, the measured performance of each classifier reflects both its intrinsic discrimination power and the reconstruction efficiency of the corresponding algorithm.

Figure 2 shows the jet (left panel) and electron (right panel) misidentification probability as a function of the genuine τ_h efficiency. The figures show that intrinsic efficiency of the HPS reconstruction is about 75% and can be recovered with the use of either CHS or PUPPI jets. From the point of view of jet rejection, the best performance is achieved by CHS+PNet followed by HPS+DeepTau for the high purity regime used in many analyses. Conversely, UParT achieves the best performance in electron discrimination, followed by HPS+DeepTau in high-rejection mode, where its efficiency is not limited by the inefficiency of the HPS reconstruction.

The Venn diagrams in Fig. 3 illustrate the overlap and complementarity among τ_h candidates reconstructed with the HPS+DeepTau, CHS+PNet, and PUPPI+UParT algorithms. The Medium

PoS(EPS-HEP2025)660

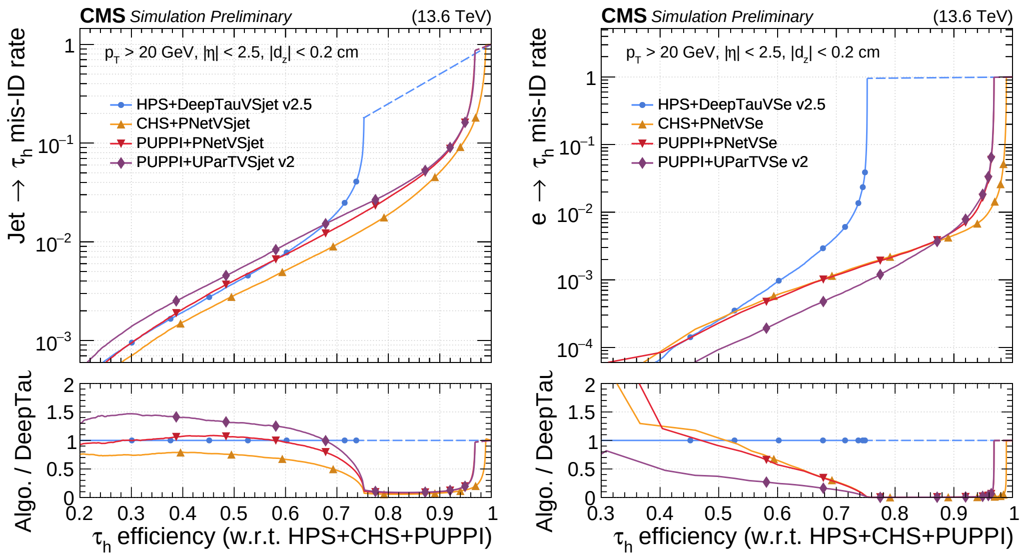

Figure 2: Jet (left) and electron (right) misidentification probability versus genuine τ_h identification efficiency for HPS+DeepTau (blue, circle), CHS+PNet (orange, triangle up), PUPPI+PNet (red, triangle down), and PUPPI+UParT (purple, diamond) algorithms [15]. The dots on the curves represent the working points defined for the discriminants, corresponding to specific fixed τ_h efficiencies.

working point is applied for the D_{jet} discriminator, while the VVVLoose and Loose working points are used for D_e and D_μ, respectively (refer to Ref. [15] for the working point definition). The left diagram shows genuine τ_h candidates, whereas the right one displays jets misidentified as τ_h. The diagrams indicate that CHS+PNet and PUPPI+UParT recover 20–30% of genuine τ_h candidates that are not reconstructed by the HPS algorithm or identified by DeepTau; however, this comes at the cost of an increased jet misidentification rate. Additional studies also show that the decay mode assignment accuracy improves with the new methods [15], at the cost of not knowing the τ_h decay products identified by HPS.

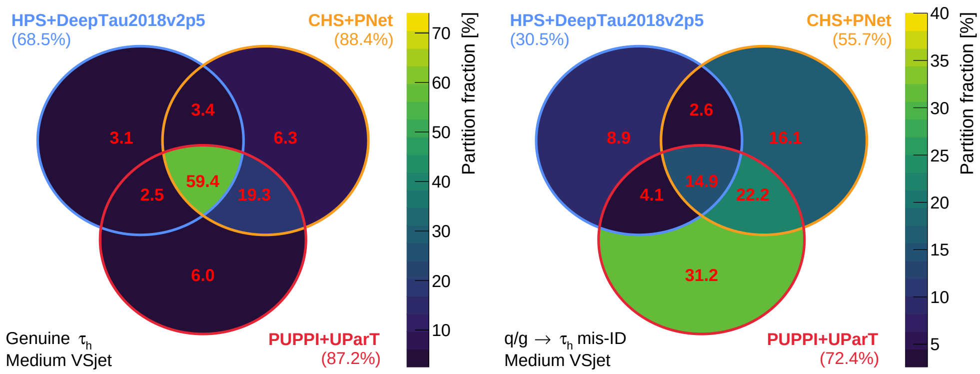

Figure 3: Venn diagrams illustrating the overlap and complementarity between τ_h candidates from the HPS+DeepTau (blue circle), CHS+PNet (orange circle), PUPPI+UParT (red circle) algorithms [15]. The red number and fill color of each partition indicate the fraction of candidates it contains relative to the union of all partitions in the diagram. While the left diagram shows genuine τ_h candidates, the right one shows jets misidentified as τ_h.

PoS(EPS-HEP2025)660

Finally, the algorithms are applied to collision data recorded during 2024. The data-to-simulation agreement before full calibration is shown in Fig. 4. It is evident that PNet provides the best rejection of the W + jets background among the different taggers, although it exhibits a higher contamination from misidentified leptons. The bottom-right plot demonstrates that combining PNet D_{jet} with DeepTau $D_{e/\mu}$ achieves the overall best performance, as evidenced by the suppression of the $Z \to \ell\ell$ peak with respect to the PNet-only figure. Notably, the plot obtained with DeepTau algorithm is the one providing the best data-to-simulation agreement thanks to the use of domain adaptation techniques.

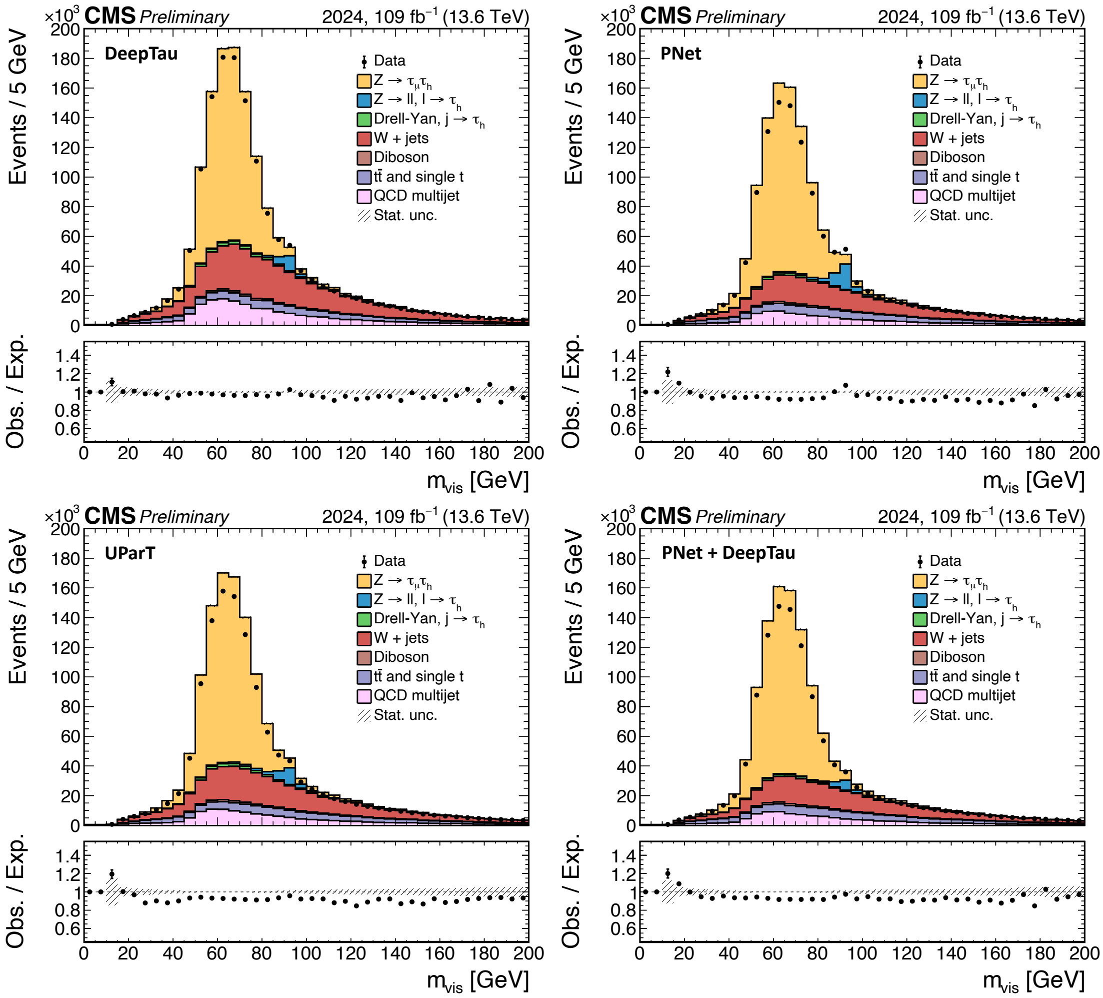

Figure 4: Data-to-simulation agreement of the visible mass using different τ_h identification algorithms [16]: DeepTau (top-left), PNet (top-right), UParT (bottom-left), PNet+DeepTau (bottom-right). The data correspond to an integrated luminosity of 109 fb^{-1}, collected by the CMS experiment in 2024. The event selection carried out aims at keeping the same yield for the $Z \to \tau_\mu \tau_h$ process in order to fairly compare the background rejections for fixed genuine τ_h efficiency. In the PNet+DeepTau plot, the baseline is the PNet selection with the addition of the DeepTau Tight requirement for the D_μ discriminator on τ_h candidates that are also reconstructed with HPS.

PoS(EPS-HEP2025)660

4. Summary

An overview of the currently available techniques for reconstructing and identifying τ_h candidates with the CMS experiment has been presented. Their respective strengths, limitations, and complementarities have been highlighted. Since the algorithms are optimized differently, combining them provides the most comprehensive and effective strategy for τ_h identification to date.

References

[1] CMS Collaboration, *The CMS Experiment at the CERN LHC*, *JINST* **3** (2008) S08004. doi:10.1088/1748-0221/3/08/S08004.

[2] CMS Collaboration, "Performance of reconstruction and identification of τ leptons decaying to hadrons and ν_τ in pp collisions at $\sqrt{s}$ = 13 TeV," *JINST*, vol. 13, p. P10005, 2018. doi:10.1088/1748-0221/13/10/P10005. arXiv:1809.02816.

[3] CMS Collaboration, "Identification of hadronic tau lepton decays using a deep neural network," *JINST*, vol. 17, p. P07023, 2022. doi:10.1088/1748-0221/17/07/p07023. arXiv:2201.08458.

[4] M. Cacciari, G. P. Salam, and G. Soyez, "The anti-k_t jet clustering algorithm," *JHEP*, vol. 04, p. 063, 2008. doi:10.1088/1126-6708/2008/04/063

[5] CMS Collaboration, "Particle-flow reconstruction and global event description with the CMS detector," *JINST*, vol. 12, no. 10, p. P10003, 2017. doi:10.1088/1748-0221/12/10/P10003

[6] CMS Collaboration, "Identification of tau leptons using a convolutional neural network with domain adaptation in the CMS experiment," CMS Physics Analysis Summary, 2024. CMS-PAS-TAU-24-001.

[7] CMS Collaboration, "Pileup mitigation at CMS in 13 TeV data," *JINST*, vol. 15, p. P09018, 2020. doi:10.1088/1748-0221/15/09/P09018.

[8] D. Bertolini, P. Harris, M. Low, and N. Tran, "Pileup per particle identification," *JHEP*, vol. 10, p. 059, 2014. doi:10.1007/JHEP10(2014)059.

[9] CMS Collaboration, "Optimizing the pileup per particle identification algorithm in the context of τ_h lepton identification in Run 3," CMS Detector Performance Summary, 2024. CMS-DP-2024-043.

[10] H. Qu and L. Gouskos, "ParticleNet: Jet Tagging via Particle Clouds," *Phys. Rev. D*, vol. 101, no. 5, p. 056019, 2020. doi:10.1103/PhysRevD.101.056019.

[11] CMS Collaboration, "Jet energy scale and resolution of jets with ParticleNet p_T regression using Run 3 data collected by the CMS experiment in 2022 and 2023 at $\sqrt{s}$ = 13.6 TeV," CMS Detector Performance Summary, 2024. CMS-DP-2024-064.

[12] H. Qu, C. Li, and S. Qian, "Particle Transformer for Jet Tagging," arXiv:2202.03772.

PoS(EPS-HEP2025)660

[13] CMS Collaboration, "A unified approach for jet tagging in Run 3 at $\sqrt{s} = 13.6$ TeV in CMS," CMS Detector Performance Summary, 2024. CMS-DP-2024-066.

[14] A. Stein, et al., "Improving robustness of jet tagging algorithms with adversarial training," *Comput. Softw. Big Sci.*, vol. 6, p. 7, 2022. doi:10.1007/s41781-022-00087-1.

[15] CMS Collaboration, "Comparison of the performance of tau reconstruction and identification algorithms in Run 3," CMS Detector Performance Summary, 2025. CMS-DP-2025-073.

[16] CMS Collaboration, "Validation of tau identification algorithms in Run 3 data and simulation," CMS Detector Performance Summary, 2025. CMS-DP-2025-074.

PoS(EPS-HEP2025)660